

TeV-PeV Neutrinos from Giant Flares of Magnetars and the Case of SGR 1806-20

Kunihiro Ioka,¹ Soebur Razzaque,² Shiho Kobayashi^{1,2}, and Peter Mészáros^{1,2}

ABSTRACT

We estimate the high energy neutrino flux from the giant flare of SGR 1806-20 on December 27, 2004, which irradiated Earth with a gamma-ray flux $\sim 10^4$ times larger than the most luminous gamma-ray bursts (GRBs) ever detected. The Antarctic Cherenkov neutrino detector AMANDA was on-line during the flare, and may either have detected high energy neutrinos for the first time from a cosmic point source, or put constraints on the flare mechanism of magnetars. If TeV neutrinos are detected, one would expect also detectable EeV cosmic rays and possibly TeV gamma-ray emission in coincidence.

Subject headings: cosmic rays — gamma rays: bursts — gamma rays: theory — stars: individual (SGR1806-20) — stars: neutron

1. Introduction

The giant flare of SGR 1806-20 on December 27, 2004 was the brightest cosmic transient to date, emitting gamma-rays for ~ 0.1 sec with flux ~ 10 erg s $^{-1}$ cm $^{-2}$ (Terasawa et al. 2005; Hurley et al. 2005; Mazets et al. 2005; Palmer et al. 2005). If a comparable energy was emitted as high energy neutrinos, they should have been detected for the first time by current neutrino observatories such as AMANDA (Ahrens et al. 2002). In this Letter we calculate the expected high energy neutrino flux from giant flares in Soft Gamma-ray Repeaters (SGRs) such as SGR 1806-20, and argue that the neutrino flux is indeed either detectable, or its absence provides important constraints on the flare mechanism (see Zhang et al. (2003) for high energy neutrinos from quiescent magnetars).

¹Physics Department and Center for Gravitational Wave Physics, 104 Davey Laboratory, Pennsylvania State University, University Park, PA 16802

²Department of Astronomy and Astrophysics, 525 Davey Laboratory, Pennsylvania State University, University Park, PA 16802

SGRs are a type of extreme X-ray pulsars, repeatedly emitting ~ 0.1 sec bursts of soft gamma-rays. Giant flares are more energetic events, which have been recorded from three of four known SGRs with the December 27 event being the third one. SGRs are most likely magnetars, i.e., highly magnetized neutron stars (Thompson & Duncan 1995, 2001). In this model giant flares result from a global magnetic rearrangement of the crust or even the entire interior (e.g., Ioka 2001).

Giant flares have many similarities to cosmological gamma-ray bursts (GRBs). Long duration GRBs are thought to arise from relativistic jets interacting with themselves for prompt GRBs, and subsequently with a circumburst medium for the longer wavelength afterglows (e.g., Zhang & Mészáros 2004). In a similar manner, the detected radio afterglows of SGRs imply the presence of relativistic outflows (Frail, Kulkarni & Bloom 1999; Cameron et al. 2005; Gaensler et al. 2005), and the huge flare luminosities also lead to relativistic fireballs (Huang, Dai & Lu 1998; Thompson & Duncan 2001; Nakar, Piran & Sari 2005). In particular, the minimum energy of the radio afterglow is larger than the kinetic energy of e^\pm pairs that survive annihilation, implying the presence of baryons in fireballs like GRBs (Nakar, Piran & Sari 2005). Relativistic baryons are likely to cause shocks, leading to Fermi accelerated protons, and to high energy neutrinos via $p\gamma$ (Waxman & Bahcall 1997) and pp interactions (Paczynski & Xu 1994). The accelerated protons in GRBs may also explain the observed ultrahigh energy cosmic rays (Waxman 1995; Vietri 1995; Ioka, Kobayashi, & Mészáros 2004).

In contrast to GRBs, however, the baryon load in giant SGR flares is less constrained (see § 2), mainly because the flare spectrum may be thermal (Hurley et al. 2005) or nonthermal (Mazets et al. 2005; Palmer et al. 2005). Since the neutrino fluxes depend on the baryon load, neutrinos can be a probe of the baryon load as well as the flare mechanism. In § 2 we discuss typical fireball models for SGR 1806-20 and in § 3 we estimate the expected high energy neutrino fluxes for these models. The implications are discussed in § 4.

2. Typical fireball models for SGR 1806-20

The giant flare of SGR 1806-20 on December 27, 2004 radiated a gamma-ray energy $E_\gamma \sim 3 \times 10^{46} E_{\gamma,46.5}$ erg during a time of $t_0 \sim 0.1 t_{0,-1}$ sec (Terasawa et al. 2005).³ The total luminosity was $L_0 \sim L_\gamma/\xi_\gamma \sim 3 \times 10^{47} L_{0,47.5}$ erg s⁻¹ for a conversion efficiency ξ_γ of total energy into gamma-ray. If such energy is released near a neutron star (radius $r_0 \sim$

³We adopt $d = 10d_1$ kpc for the distance to SGR 1806-20 though it is controversial (Cameron et al. 2005; Corbel & Eikenberry 2004).

$10^6 r_{0,6}$ cm), e^\pm pair production creates an optically thick fireball with an initial temperature (Paczynski 1986; Goodman 1986)

$$T_0 \sim \left(\frac{L_0}{4\pi r_0^2 c a} \right)^{1/4} \sim 300 L_{0,47.5}^{1/4} r_{0,6}^{-1/2} \text{ keV}, \quad (1)$$

where $a = \pi^2 k^4 / 15 \hbar^3 c^3 = 7.6 \times 10^{-15}$ erg cm $^{-3}$ K $^{-4}$ is the radiation density constant. As the fireball expands under its own pressure, the Lorentz factor increases as $\Gamma \propto r$ and the comoving temperature drops as $T \propto r^{-1}$. The subsequent evolution depends on the baryon load parametrized by a dimensionless entropy $\eta = L_0 / \dot{M} c^2$ (Shemi & Piran 1990). If the fireball is baryon-rich, $\eta < \eta_*$, where η_* is a critical entropy (Mészáros & Rees 2000)

$$\eta_* = \left(\frac{L_0 \sigma_T}{4\pi m_p c^3 r_0} \right)^{1/4} \sim 100 L_{0,47.5}^{1/4} r_{0,6}^{-1/4}, \quad (2)$$

a photosphere appears in the coasting phase and almost all the energy goes into the kinetic luminosity of the outflow $L_{\text{kin}} \sim L_0$, while a photosphere appears in the acceleration phase if $\eta > \eta_*$. We can derive

$$\begin{aligned} \Gamma_f &= \min[\eta, \eta_*], \quad r_{\text{ph}}/r_0 = \max[\eta_*(\eta/\eta_*)^{-3}, \eta_*(\eta/\eta_*)^{-1/3}], \\ L_{\text{kin}}/L_0 &= \min[1, \eta_*/\eta], \quad L_{\text{ph}}/L_0 = \min[(\eta/\eta_*)^{8/3}, 1], \quad T_{\text{ph}}/T_0 = \min[(\eta/\eta_*)^{8/3}, 1], \end{aligned} \quad (3)$$

where the first (second) value in the bracket is for $\eta < \eta_*$ ($\eta > \eta_*$), Γ_f is the final Lorentz factor, a thermal photosphere at radius r_{ph} has a luminosity L_{ph} with an observed temperature T_{ph} , and we neglect finite shell effects for simplicity (Mészáros et al. 2002). The above relations hold provided the fireball is not too baryon-poor, $\eta > \eta_\pm \sim 10^5 L_{47.5}^{1/4} r_{0,6}^{1/2}$ (Mészáros & Rees 2000).

Internal shocks in a variable outflow with $\Gamma = 10^2 \Gamma_2$ are expected to occur at radii

$$r_s \simeq 2\Gamma^2 c \Delta t \sim 6 \times 10^{13} \Gamma_2^2 \Delta t_{-1} \text{ cm} \quad (4)$$

where $\Delta t = 10^{-1} \Delta t_{-1}$ s is the variability timescale. The minimum value is $\Delta t \sim r_0/v_A \sim 3 \times 10^{-5}$ s since the Alfvén velocity in the magnetosphere is $v_A \sim c$, which is consistent with the initial rise time $\lesssim 0.3$ ms (Terasawa et al. 2005; Palmer et al. 2005). If shocks occur above the photosphere, i.e., $\eta > \eta_s = 10 L_{0,47.5}^{1/5} \Delta t_{-1}^{-1/5}$, nonthermal radiation is produced. The nonthermal shock luminosity $L_s = \xi_s L_{\text{kin}}$ dominates the photospheric luminosity L_{ph} if $\eta < 100 \eta_{*,2} \xi_s^{3/8}$, where ξ_s is the conversion efficiency of kinetic energy into photons.

Two typical scenarios are possible for the December 27 flare. The first one is a baryon-poor scenario, e.g. $\eta \sim 10^4 > \eta_*$, where the photosphere is in the acceleration phase. Most of the energy is radiated as photospheric emission, which may explain the thermal spectrum

with temperature $T_\gamma \sim 175 \pm 25$ keV observed by Hurley et al. (2005). The remaining kinetic energy is $\eta/\eta_* \sim 10^2$ times smaller than the radiation energy, which is also implied by the radio afterglow of SGR 1806-20, if we use typical parameters inferred from GRB afterglow fittings $\xi_e \sim 0.1$, $\xi_B \sim 0.01$ and $n \sim 1 \text{ cm}^{-3}$ (Nakar, Piran & Sari 2005; Wang et al. 2005).

The second is a baryon-rich scenario, e.g. with $\eta \sim 10 < \eta_*$. The observed thermal radiation L_γ can be explained by a thermalized shock luminosity $L_s = \xi_s L_{\text{kin}}$, if shocks occurred right below the photosphere (Rees & Mészáros 2004). The remaining kinetic energy is $(1 - \xi_s)/\xi_s \sim 10\xi_{s,-1}^{-1}$ times larger than the radiation energy, so that the observed radio afterglow may require a jet configuration ($\theta \lesssim 0.1$) or atypical model parameters (high ambient density n and low ξ_e or ξ_B). However a jet may be implied by the elliptical image and polarization of the radio afterglow (Gaensler et al. 2005) as well as the light curve of the giant flare that is well fitted by emission from a relativistic jet (Yamazaki et al. 2005). Atypical parameters may be also suggested by the rapid decay of the radio afterglow (Cameron et al. 2005). Thus this model may also be viable.

The actual spectrum of the November 27 flare, however, may be nonthermal (Palmer et al. 2005; Mazets et al. 2005). At least a portion of the giant flare may be nonthermal, since Hurley et al. (2005) determined the spectrum with low time resolution. A previous giant flare in SGR 0526-66 may also have had a nonthermal spectrum (Fenimore, Klebesadel, & Laros 1996). If giant flares are observed as short GRBs, their spectra are also likely nonthermal (Fenimore, Klebesadel, & Laros 1996; Nakar et al. 2005). A nonthermal flare component may arise in a baryon-rich model $\eta \gtrsim 10$, since internal shocks extending above the photosphere naturally produce nonthermal emission. The characteristic synchrotron frequency $\epsilon_m = \Gamma \gamma_m^2 \hbar q B / m_e c$ in internal shocks can be estimated as

$$\epsilon_m \sim 300 \xi_B^{1/2} \xi_e^{3/2} L_{\gamma,47.5}^{1/2} \Gamma_1^{-2} \Delta t_{-1}^{-1} \text{ keV}, \quad (5)$$

where a fraction ξ_e of the internal energy goes into electrons ($\gamma_m \sim \xi_e m_p / m_e$) and a fraction ξ_B goes into the magnetic field, $4\pi r_s^2 c \Gamma^2 B^2 / 8\pi = \xi_B L_\gamma / \xi_e$. Note that this synchrotron emission is not thermalized above the photosphere.

3. Proton interactions and neutrinos

According to § 2, we choose the particular parameters for the two typical models as

baryon – poor (BP) : $\eta \sim 10^4$, $L_{\text{kin}} \sim 10^{-2} L_\gamma \sim 10^{45.5} \text{ erg s}^{-1}$, $\Gamma \sim 100$, $\Delta t \sim 10^{-4} \text{ s}$,

baryon – rich (BR) : $\eta \sim 10$, $L_{\text{kin}} \sim 10 L_\gamma \sim 10^{48.5} \text{ erg s}^{-1}$, $\Gamma \sim 10$, $\Delta t \sim 10^{-1} \text{ s}$.

We set Δt in the baryon-poor model to maximize neutrino events, which turn out to be undetectable. In the baryon-poor (baryon-rich) model internal shocks take place outside (inside) the photospheric radius ($\tau_{\text{Th}} \sim 1$). Since the internal shocks are mildly relativistic, protons are expected to be accelerated to a power law distribution, $dn_p/d\epsilon_p \propto \epsilon_p^{-2}$ (Waxman & Bahcall 1997; Waxman 1995; Vietri 1995). High energy protons may then interact with photons ($p\gamma$) or with other cold protons (pp) to produce neutrinos mostly through pion decays. The maximum shocked proton energy in the comoving equipartition magnetic field: $B' = \sqrt{8\pi n'_p m_p c^2 \xi_B \xi_i}$, where n'_p is the comoving baryon number density, is limited by the system size and synchrotron losses. By equating the acceleration time $t'_{\text{acc}} \sim \epsilon'_p/cqB'$ to the shorter of the comoving time $t'_{\text{com}} \sim r_s/\Gamma c$ and the synchrotron cooling time $t'_{\text{syn}} \sim 6\pi m_p^4 c^3 / \sigma_T m_e^2 \epsilon'_p B'^2$ we find the maximum proton energy in the lab-frame as

$$\epsilon_{p,\text{max}} \sim \begin{cases} 4 \times 10^{16} (\xi_{B,-2} \xi_{i,-1} L_{\text{kin},45.5})^{1/2} \Gamma_2^{-1} \text{ eV} & (\text{BP}) \\ 7 \times 10^{18} (\xi_{B,-2} \xi_{i,-1} L_{\text{kin},48.5})^{-1/4} \Gamma_1^{5/2} \Delta t_{-1}^{1/2} \text{ eV} & (\text{BR}), \end{cases} \quad (6)$$

where a fraction $\xi_i \sim 0.1 \xi_{i,-1}$ of the kinetic energy goes into the internal energy. Note that t'_{com} is smaller (greater) than t'_{syn} in the baryon-poor (baryon rich) model.

The comoving baryon density in the two models is

$$n'_p = \frac{L_{\text{kin}}}{4\pi r_s^2 \Gamma^2 m_p c^3} \sim \begin{cases} 2 \times 10^{11} L_{\text{kin},45.5} \Gamma_2^{-6} \Delta t_{-4}^{-2} \text{ cm}^{-3} & (\text{BP}) \\ 2 \times 10^{14} L_{\text{kin},48.5} \Gamma_1^{-6} \Delta t_{-1}^{-2} \text{ cm}^{-3} & (\text{BR}). \end{cases} \quad (7)$$

The accelerated proton flux that would be measured at Earth, if they were to reach us in a straight line before converting to neutrinos is

$$\Phi_p = \frac{\xi_i L_{\text{kin}}}{4\pi d^2 \epsilon_p^2} \sim \begin{cases} 20 (\epsilon_p/\text{GeV})^{-2} \xi_{i,-1} L_{\text{kin},45.5} d_1^{-2} \text{ GeV}^{-1} \text{ cm}^{-2} \text{ s}^{-1} & (\text{BP}) \\ 2 \times 10^4 (\epsilon_p/\text{GeV})^{-2} \xi_{i,-1} L_{\text{kin},48.5} d_1^{-2} \text{ GeV}^{-1} \text{ cm}^{-2} \text{ s}^{-1} & (\text{BR}). \end{cases} \quad (8)$$

A fraction of this proton flux will be converted to neutrinos depending on the opacity of $p\gamma$ and pp interactions in the fireball.

The photospheric thermal radiation bathes the ejecta at the internal shock region (which also radiates), so that accelerated protons interact with photons (using the observed T_γ) of comoving energy

$$\epsilon'_\gamma \sim T_\gamma/\Gamma \sim \begin{cases} 2 \Gamma_2^{-1} \text{ keV} & (\text{BP}) \\ 20 \Gamma_1^{-1} \text{ keV} & (\text{BR}) \end{cases} \quad (9)$$

and can produce pions if the observed proton energy is

$$\epsilon_p \sim \frac{0.3 \Gamma^2 \text{ GeV}^2}{\epsilon'_\gamma} \sim \begin{cases} 2 \times 10^{16} \Gamma_2^2 \epsilon_{\gamma,5.3}^{-1} \text{ eV} & (\text{BP}) \\ 2 \times 10^{14} \Gamma_1^2 \epsilon_{\gamma,5.3}^{-1} \text{ eV} & (\text{BR}), \end{cases} \quad (10)$$

which is below the maximum available proton energy in both the models. The density of these thermal photons at the shocks is⁴

$$n'_\gamma \sim \frac{L_\gamma}{4\pi r_s^2 \Gamma^2 c \epsilon'_\gamma} \sim \begin{cases} 7 \times 10^{18} L_{\gamma,47.5} \epsilon_{\gamma,5.3}^{-1} \Gamma_2^{-5} \Delta t_{-4}^{-2} \text{ cm}^{-3} & (\text{BP}) \\ 7 \times 10^{17} L_{\gamma,47.5} \epsilon_{\gamma,5.3}^{-1} \Gamma_1^{-5} \Delta t_{-1}^{-2} \text{ cm}^{-3} & (\text{BR}). \end{cases} \quad (11)$$

The corresponding optical depth to $p\gamma$ interactions is then

$$\tau_{p\gamma} \sim \frac{\sigma_{p\gamma} n'_\gamma r_s}{\Gamma} \sim \begin{cases} 2 L_{\gamma,47.5} \epsilon_{\gamma,5.3}^{-1} \Gamma_2^{-4} \Delta t_{-4}^{-1} & (\text{BP}) \\ 20 L_{\gamma,47.5} \epsilon_{\gamma,5.3}^{-1} \Gamma_1^{-4} \Delta t_{-1}^{-1} & (\text{BR}), \end{cases} \quad (12)$$

where $\sigma_{p\gamma} \sim 5 \times 10^{-28} \text{ cm}^2$ is the cross-section at the Δ resonance.

Protons lose $\sim 20\%$ of their energy at each $p\gamma$ interaction, dominated by the Δ resonance. Approximately half of the pions are charged and decay into high energy neutrinos $\pi^+ \rightarrow \mu^+ + \nu_\mu \rightarrow e^+ + \nu_e + \bar{\nu}_\mu + \nu_\mu$, with the energy distributed roughly equally among the decay products. Thus the neutrino energy is $\sim 5\%$ of the proton energy. From equation (10), we find the typical neutrino energy expected from the $p\gamma$ interactions with thermal photons as

$$\epsilon_\nu \sim \frac{0.3 \Gamma^2 \text{GeV}^2}{20 \epsilon_\gamma} \sim \begin{cases} 8 \times 10^5 \Gamma_2^2 \epsilon_{\gamma,5.3}^{-1} \text{ GeV} & (\text{BP}) \\ 8 \times 10^3 \Gamma_1^2 \epsilon_{\gamma,5.3}^{-1} \text{ GeV} & (\text{BR}). \end{cases} \quad (13)$$

The corresponding monoenergetic neutrino flux at Earth (equal for ν_μ , ν_τ and ν_e after oscillations in vacuum where $\bar{\nu}_\mu$ created from π^+ decay is transformed to ν_τ) can be found from equation (8) as

$$\begin{aligned} \Phi_{\nu,p\gamma} &= \min(1, \tau_{p\gamma}) \frac{0.2}{8} \frac{\xi_i L_{\text{kin}}}{4\pi d^2 \epsilon_\nu^2} \\ &\sim \begin{cases} 7 \times 10^{-13} \xi_{i,-1} L_{\text{kin},45.5} \epsilon_{\gamma,5.3}^2 d_1^{-2} \Gamma_2^{-4} \text{ GeV}^{-1} \text{ cm}^{-2} \text{ s}^{-1} & (\text{BP}) \\ 7 \times 10^{-6} \xi_{i,-1} L_{\text{kin},48.5} \epsilon_{\gamma,5.3}^2 d_1^{-2} \Gamma_1^{-4} \text{ GeV}^{-1} \text{ cm}^{-2} \text{ s}^{-1} & (\text{BR}), \end{cases} \end{aligned} \quad (14)$$

where in both the cases $\min(1, \tau_{p\gamma}) = 1$ from equation (12). Note that the synchrotron and inverse Compton losses of π^+ and μ^+ are negligible for our models.

In addition to $p\gamma$ interactions, shock accelerated protons may also undergo pp interactions with cold protons in the ejecta and produce π^\pm . The opacity for pp interactions is about $\tau_{pp} \sim \sigma_{pp} n'_p r_s / \Gamma \sim 0.6 L_{\text{kin},48.5} \Gamma_1^{-5} \Delta t_{-1}^{-1} \sim 0.1 \tau_{\text{Th}}$ for an average pp cross-section of $\sigma_{pp} \sim 6 \times 10^{-26} \text{ cm}^2$ in the TeV-PeV energy range. We calculate the neutrino flux from π^\pm decays as (Razzaque, Mészáros, & Waxman 2003)

$$\Phi_{\nu,pp} = \min(1, \tau_{pp}) \int^{\epsilon_{p,\text{max}}} \Phi_p M_\nu(\epsilon_p) d\epsilon_p, \quad (15)$$

⁴Below the photosphere the photon density could be larger than this estimate.

where the neutrino multiplicity from pp interactions in units of GeV^{-1} is given by

$$M_\nu(\epsilon_p) = \frac{7}{4} \left(\frac{\epsilon_\nu}{\text{GeV}} \right)^{-1} \left[\frac{1}{2} \ln \left(\frac{10^{11} \text{GeV}}{\epsilon_p} \right) \right]^{-1} \Theta \left(\frac{1}{4} \frac{m_\pi}{\text{GeV}} \gamma_{\text{cm}} \leq \frac{\epsilon_\nu}{\text{GeV}} \leq \frac{1}{4} \frac{\epsilon_p}{\text{GeV}} \right), \quad (16)$$

γ_{cm} is the Lorentz factor of the pp center of mass in the lab-frame and Θ is a step function. Note that the flux is given for muon (anti muon) neutrinos. Electron and tau (and their anti) neutrino fluxes would be the same on Earth. We may fit the pp muon neutrino flux for $\tau_{pp} < 1$ by

$$\Phi_{\nu,pp} = \left[330 + 30 \ln \left(\frac{\epsilon_\nu}{\text{GeV}} \right) \right] \left(\frac{\epsilon_\nu}{\text{GeV}} \right)^{-2} \xi_{i,-1} L_{\text{kin},48.5}^2 d_1^{-2} \Gamma_1^{-5} \Delta t_{-1}^{-1} \text{GeV}^{-1} \text{cm}^{-2} \text{s}^{-1}. \quad (17)$$

For the baryon-poor model with optically thin internal shocks, an additional neutrino component may arise due to $p\gamma$ interactions with non-thermal synchrotron photons, but this latter flux component is undetectably low and is ignored. Next we calculate the expected neutrino events at Earth.

4. Neutrino events in AMANDA

SGR1806-20 is located in the southern sky at a declination of -20° . We have calculated the probability to detect muon neutrinos with the AMANDA detector, located at the South pole at a depth of 1 km, by using a code which propagates neutrinos through Earth and calculates the interaction rate in ice near the vicinity of the detector (Razzaque, Mészáros, & Waxman 2004). The resulting probability may be fitted in the TeV-EeV energy range with a broken power-law as

$$P(\epsilon_\nu) = 7 \times 10^{-5} (\epsilon_\nu / 10^{4.5} \text{GeV})^\beta, \quad (18)$$

where $\beta = 1.35$ for $\epsilon_\nu < 10^{4.5}$ GeV while $\beta = 0.55$ for $\epsilon_\nu > 10^{4.5}$ GeV. Using a geometrical detector area of $A_{\text{det}} = 0.03 \text{ km}^2$ and the flare duration $t_0 = 0.1 \text{ s}$, the number of muon events from $p\gamma$ neutrinos (ν_μ) of energy given in equation (13) is

$$\begin{aligned} N_{\mu,p\gamma} &= A_{\text{det}} t_0 P(\epsilon_\nu) \epsilon_\nu \Phi_{\nu,p\gamma} \\ &\sim \begin{cases} 0.007 \min(1, \tau_{p\gamma}) \xi_{i,-1} L_{\text{kin},45.5}^2 d_1^{-2} (\epsilon_{\gamma,5.3}^{-1} \Gamma_2^2)^{\beta-1} A_{\text{det},-1.5} t_{0,-1} & (\text{BP}) \\ 20 \min(1, \tau_{p\gamma}) \xi_{i,-1} L_{\text{kin},48.5}^2 d_1^{-2} (\epsilon_{\gamma,5.3}^{-1} \Gamma_1^2)^{\beta-1} A_{\text{det},-1.5} t_{0,-1} & (\text{BR}) \end{cases} \end{aligned} \quad (19)$$

On the other hand, the number of muon events from pp neutrinos would be

$$\begin{aligned} N_{\mu,pp} &= 2 A_{\text{det}} t_0 \int_{\text{TeV}}^{\text{PeV}} P(\epsilon_\nu) \Phi_{\nu,pp} d\epsilon_\nu \\ &\sim \begin{cases} 3 \times 10^{-6} \xi_{i,-1} L_{\text{kin},45.5}^2 d_1^{-2} \Gamma_2^{-5} \Delta t_{-4}^{-1} A_{\text{det},-1.5} t_{0,-1} & (\text{BP}) \\ 300 \xi_{i,-1} L_{\text{kin},48.5}^2 d_1^{-2} \Gamma_1^{-5} \Delta t_{-1}^{-1} A_{\text{det},-1.5} t_{0,-1} & (\text{BR}) \end{cases} \end{aligned} \quad (20)$$

where we use equation (17) and note that Cherenkov detectors do not distinguish between ν_μ and $\bar{\nu}_\mu$ flavors. The difference of the arrival time between neutrinos and gamma-rays would be within $\sim t_0 \sim 0.1$ s. Neutrinos can precede gamma-rays if internal shocks occur deeply inside the photosphere.

In Figure 1, based on similar calculations, we show the parameter space where AMANDA and the future detector ICECUBE ($A_{\text{det}} = 1 \text{ km}^2$) (Ahrens et al. 2004) can detect more than one muon event in the plane of the baryon load η and the variability timescale Δt . (Note that background events are negligible.) Baryons are rich (poor) for $\eta \lesssim 10^2$ ($\eta \gtrsim 10^2$) while the corresponding Lorentz factor is $\Gamma \sim \eta$ ($\Gamma \sim 10^2$) in equation (3). We can see that TeV-PeV neutrinos may have been already detected by AMANDA if the giant flare is baryon-rich ($\eta \lesssim 30$), while a nondetection would suggest a baryon-poor fireball. This offers the exciting prospect of gaining independent information about the baryon load or the bulk Lorentz factor of the fireball, the efficiency of proton injection and energy dissipation in shocks and the variability timescale associated with the flare trigger. Such parameters would constrain the energetics and the radiation mechanisms inferred from electromagnetic observations.

If the neutrinos from this flare are detected by AMANDA, one would expect ICECUBE to be able to detect less energetic flares in this and other galactic SGRs. One can show that the baryon-rich model with a flare $\sim 10^{-3}$ times smaller than that considered here can produce about one event in ICECUBE, and the rate of such flares is about $\sim 1/10$ yr.

Since sedimentation due to gravity causes heavier elements to stratify down, the surface tends to consist of lighter elements (Alcock & Illarionov 1980). An absorption feature in bursts from SGR 1806-20 was interpreted as due to proton cyclotron lines (Ibrahim, Swank, & Parke 2003; Ho & Lai 2001). However the magnetar surface may not contain hydrogen since hydrogen could burn very fast (Chang, Arras, & Bildsten 2004). If a fireball contains some heavy nuclei, photo disintegration processes with thermal photons may substantially reduce the maximum energy of the nuclei (Puget, Stecker, & Bredekamp 1976). A detailed calculation requiring a Monte Carlo simulation is out of the scope of this Letter. Here we present qualitative remarks if a nucleus of arbitrary mass number A and charge Z survives photo disintegration while being accelerated in the internal shocks. Their maximum energy would be $\propto Z$ for $t'_{\text{com}} < t'_{\text{syn}}$ and $\propto A^2 Z^{-3/2} \sim Z^{1/2}$ for $t'_{\text{com}} > t'_{\text{syn}}$ in equation (6). The threshold energy of nuclei for the pion production is $\sim A$ times equation (10). The pions decay into neutrinos and the typical neutrino energy is almost the same as equation (13). Since the neutrino energy is the same, the neutrino flux is the same as equation (14). (Note that the optical depth for $\sim A$ pion production by nuclei is also the same as equation (12) because the photomeson cross-section is $\sim A\tau_{p\gamma}$.) Therefore the number of muon events in

equation (19) does not change much.

External shocks that produce the radio afterglows may also accompany neutrino emissions. A simple application of the GRB afterglow (Wang et al. 2005), however, shows that the typical synchrotron frequency is too low to make the $p\gamma$ interactions.

Neutrons produced by $p\gamma$ interactions can reach us in a straight line without decay if their energy is larger than $\sim 10^{18}$ eV (e.g., Ioka, Kobayashi, & Mészáros 2004), and may be observed as coincident cosmic rays. Since $\epsilon_p \sim 10^{18}$ eV protons interact with $\sim 40\Gamma_1^2\epsilon_{p,18}^{-1}$ eV flare photons, the $p\gamma$ optical depth is about $\tau_{p\gamma} \sim 8 \times 10^{-7}L_{\gamma,47.5}\Delta t_{-1}^{-1}\epsilon_{p,18}^{-2}$ if we assume a thermal spectrum. Then the number of cosmic ray events in $A_{\text{det}} \sim 10^3$ km² detectors such as AUGER (Abraham et al. 2004) may be $N_n \sim \epsilon_p\Phi_p\tau_{p\gamma}A_{\text{det}}t_0 \sim 10\epsilon_{p,18}^{-3}\xi_{i,-1}L_{\text{kin},48.5}^2d_1^{-2}\Delta t_{-1}^{-1}$.

Neutral pions produced by $p\gamma$ and pp interactions decay into two gamma-rays with a flux and energy comparable to neutrinos. These gamma-rays might be detected by Milagro (Atkins et al. 2003) if the flare had occurred in the northern sky and if the gamma-rays escape the emission region without making pairs.

We are grateful to C. Thompson for discussions, to the referee for comments, and to TIARA-Tsinghua University for hospitality (PM). This work was supported in part by the Eberly Research Funds of Penn State and by the Center for Gravitational Wave Physics under grants PHY-01-14375 (KI,SK), NSF AST 0307376 (SR,PM) and NAG5-13286 (PM) and by NASA Swift Cycle 1 GI program (SK).

REFERENCES

Abraham, J., et al. 2004, Nucl. Instr. Meth. A, 523, 50

Ahrens, J., et al. 2002, Phys. Rev. D, 66, 012005

Ahrens, J., et al. 2004, Astropart. Phys., 20, 507

Alcock, C., & Illarionov, A. 1980, ApJ, 235, 534

Atkins, R., et al. 2003, ApJ, 595, 803

Cameron, P. B., et al. 2005, Nature, 434, 1112

Chang, P., Arras, P., & Bildsten, L. 2004, ApJ, 616, L147

Corbel, S., & Eikenberry, S. S. 2004, A&A, 419, 191

Fenimore, E. E., Klebesadel, R. W., & Laros, J. G. 1996, *ApJ*, 460, 964

Frail, D., Kulkarni, S. R. & Bloom, J. 1999, *Nature*, 398, 127

Gaensler, B. M., et al. 2005, *Nature*, 434, 1104

Goodman, J. 1986, *ApJ*, 308, L47

Ho, W. C. G., & Lai, D. 2001, *MNRAS*, 327, 1081

Huang, Y. F., Dai, Z. G., & Lu, T. 1998, *Chinese Physics Letters*, 15, 775

Hurley, K., et al. 2005, *Nature*, 434, 1098

Ibrahim, A. I., Swank, J. H., Parke, W. 2003, *ApJ*, 584, L17

Ioka, K. 2001, *MNRAS*, 327, 639

Ioka, K., Kobayashi, S., & Mészáros, P. 2004, *ApJ*, 613, L17

Mazets, E. P., et al. 2005, *astro-ph/0502541*

Mészáros, P., & Rees, M. J. 2000, *ApJ*, 530, 292

Mészáros, P., Ramirez-Ruiz, E., Rees, M. J., & Zhang, B. 2002, *ApJ*, 578, 812

Nakar, E., Piran, T., & Sari, R. 2005, *astro-ph/0502052*

Nakar, E., Gal-Yam, A., Piran, T., & Fox, D. B. 2005, *astro-ph/0502148*

Paczynski, B. 1986, *ApJ*, 308, L43

Paczynski, B., & Xu, G. 1994, *ApJ*, 427, 708

Palmer, D. M., et al. 2005, *Nature*, 434, 1107

Puget, J. L., Stecker, F. W., & Bredekamp, J. H. 1976, *ApJ*, 205, 638

Razzaque, S., Mészáros, P., & Waxman, E. 2003, *Phys. Rev. Lett.*, 90, 241103

Razzaque, S., Mészáros, P., & Waxman, E. 2004, *Phys. Rev. D*, 69, 023001

Rees, M.J. & Mészáros, P., 2004, *ApJ* in press, *astro-ph/0412702*

Shemi, A., & Piran, T. 1990, *ApJ*, 365, L55

Terasawa, T., et al. 2005, *Nature*, 434, 1110

Thompson, C., & Duncan, R. C. 1995, MNRAS, 275, 255

Thomson, C., & Duncan, R. C. 2001, ApJ, 561, 980

Wang, X. Y. et al. 2005, ApJ, 623, L29

Waxman, E. 1995, Phys. Rev. Lett., 75, 386

Waxman, E., & Bahcall, J. 1997, Phys. Rev. Lett., 78, 2292

Yamazaki, R., Ioka, K., Takahara, F., & Shibasaki, N. 2005, PASJ in press, astro-ph/0502320

Vietri, M. 1995, ApJ, 453, 883

Zhang, B., Dai, Z. G., Mészáros, P., Waxman, E., & Harding, A. K. 2003, ApJ, 595, 346

Zhang, B., & Mészáros, P. 2004, Int. J. Mod. Phys. A19, 2385

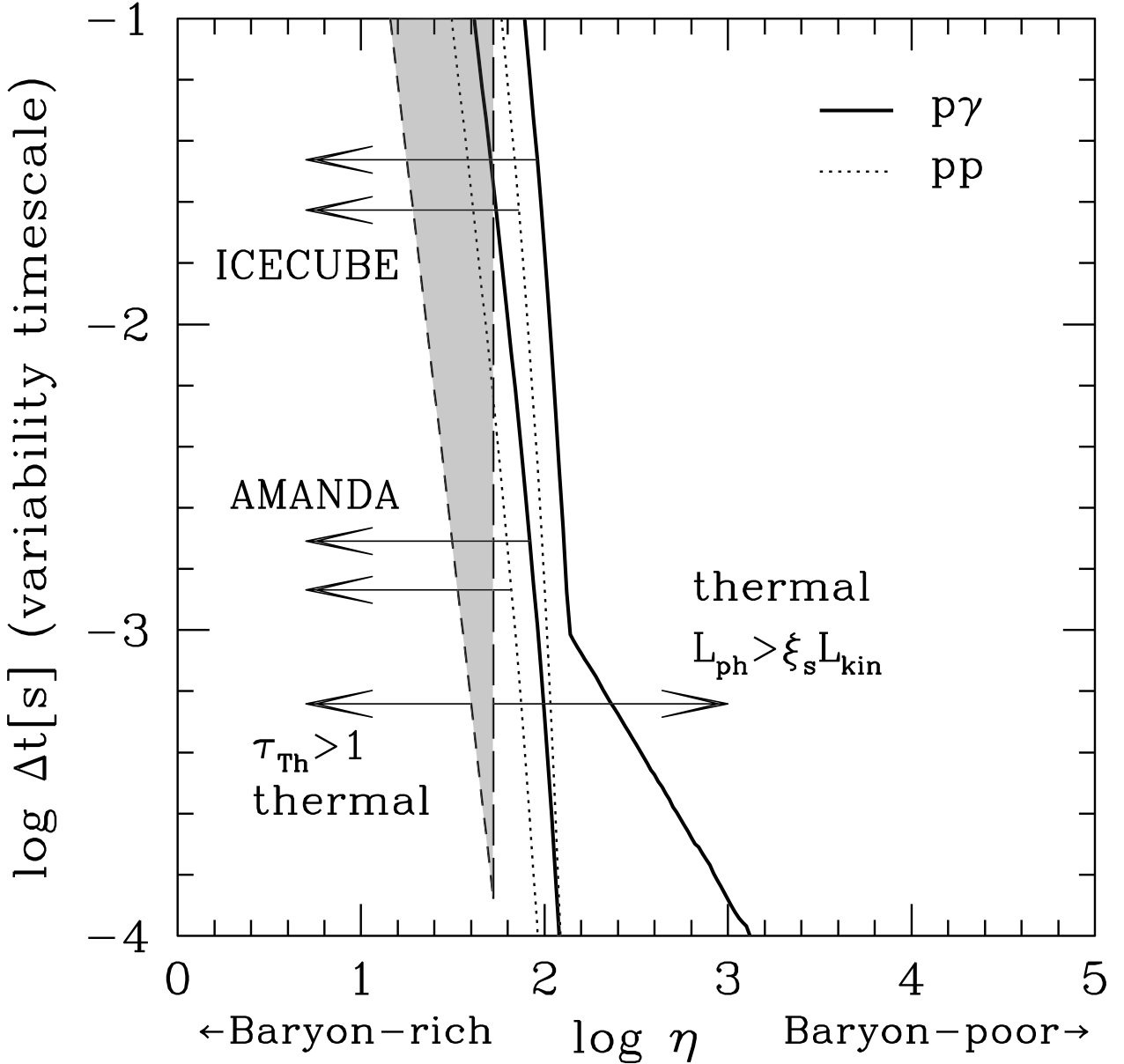


Fig. 1.— Parameter regions where AMANDA and ICECUBE can detect more than one muon event are shown in the plane of the baryon load η and the variability timescale Δt . Baryons are rich (poor) for $\eta \lesssim 10^2$ ($\eta \gtrsim 10^2$) while the corresponding Lorentz factor is $\Gamma \sim \eta$ ($\Gamma \sim 10^2$) in equation (3). Solid (dotted) lines are for $p\gamma$ (pp) neutrinos. Photospheric thermal emission dominates the nonthermal emission $L_{\text{ph}} > \xi_s L_{\text{kin}}$ on the right of the long dashed line, while internal shocks occur below the photosphere $\tau_{\text{Th}} > 1$ (also leading to a thermal spectrum) on the left of the dashed line. Thus the flare spectrum is nonthermal in the shaded region. We used a normalization $\xi_s L_{\text{kin}} + L_{\text{ph}} = L_{\gamma} = 3 \times 10^{47} \text{ erg s}^{-1}$ and adopted $\xi_B = 0.01$, $\xi_s = 0.1$ and $\xi_i = 0.1$.